

Geodetic Precession in PSR J1141–6545

A. W. Hotan

Swinburne University of Technology

ahotan@astro.swin.edu.au

M. Bailes

Swinburne University of Technology

mbailes@swin.edu.au

S. M. Ord

Swinburne University of Technology

sord@swin.edu.au

ABSTRACT

We present observations that show dramatic evolution of the mean pulse profile of the relativistic binary pulsar J1141–6545 over a period of five years. This is consistent with precession of the pulsar spin axis due to relativistic spin-orbit coupling. Observations made between 1999 and 2004 with a number of instruments at the Parkes radio telescope demonstrate a steady, secular evolution of the mean total intensity profile, which increases in width by more than 50 percent during the five year period. Analysis of the changing position angle of the linearly polarised component of the mean profile suggests that our line of sight is shifting closer to the core of the emission cone. We find that the slope of the position angle swing across the centre of the pulse steepens with time and use a simplified version of the rotating vector model to constrain the magnitude and direction of the change in our line of sight angle relative to the pulsar magnetic axis. The fact that we appear to be moving deeper into the emission cone is consistent with the non-detection of this pulsar in previous surveys.

Subject headings: Gravitation — pulsars: individual: PSR J1141–6545

1. Introduction

Soon after the discovery of the binary pulsar B1913+16 (Hulse & Taylor 1974) it was pointed out that if the pulsar’s spin axis and orbital angular momentum vector were misaligned, they should precess around their common sum on a time scale of around 300 years due to General relativistic spin-orbit coupling (Damour & Ruffini 1974; Hari Dass & Radhakrishnan 1975; Barker & O’Connell 1975; Esposito & Harrison 1975). This phenomenon is often referred to as “geodetic precession”. Because radio pulsars are thought to possess lighthouse-like beams of emission that only beam to a small fraction of the sky, such precession should lead to observable pulse shape changes once a significant fraction of the precession period has passed.

Secular changes in the mean pulse profile of PSR B1913+16 were first reported by Weisberg et al. (1989). The changes became more pronounced in later years, allowing limited modeling of the emission cone (Kramer 1998; Weisberg & Taylor 2002). The variations seen in PSR B1913+16 suggest a small misalignment angle between the spin and orbital angular momentum vectors, consistent with a natal kick being imparted to the most recently formed neutron star (Bailes 1988). Large misalignment angles raise the possibility that we might be able to, for the first time, map out the entire emission cone of a pulsar until it disappears completely from view (Kramer 1998).

For many years, PSR B1913+16 was the only binary pulsar with the right combination of relativistic parameters and an evolutionary history that would make detection of geodetic precession possible. However, shortly after geodetic precession was first hinted at, new relativistic pulsars were uncovered in pulsar surveys that would become suitable for measurements in the future. Anderson et al. (1990) discovered a near clone of the original binary pulsar in the globular cluster M15C, which although weak, might one day exhibit the phenomenon. The much closer PSR B1534+12 (Wolszczan 1990) is a relativistic pulsar in a 10 hour binary orbit that has recently been shown to exhibit pulse shape changes. These changes have been combined with polarimetric models to make the first reliable estimate of the rate at which the spin axis of the pulsar is tilting away from us (Stairs et al. 2004). Thus, measurements of geodetic precession are allowing new tests of General relativity and constraining evolutionary models (Wex et al. 2000; Konacki et al. 2003). These new tests complement the earlier pioneering work of authors such as Taylor & Weisberg (1982), that examined other aspects of the theory.

In principle, it should be possible to use the relativistic pulsars to map both shape and intensity changes across a pulsar emission cone. However, this is complicated by the fact that many of the pulsars have random variations in their total intensity because of refractive and diffractive interstellar scintillation. Pulsars with small dispersion measures (DM) often

have their fluxes change by factors of several on time scales that vary between minutes and days (Stinebring et al. 2000). However, large dispersion measure pulsars ($DM > 100 \text{ pc cm}^{-3}$) have relatively stable fluxes when observed at high frequencies ($\nu > 1.4 \text{ GHz}$) if long integration times are used and the observing system samples a large ($> 100 \text{ MHz}$) bandwidth. The discovery of a relativistic pulsar at a large DM with a rapid geodetic precession time scale might then offer the first hope of determining how rapidly pulsar emission varies in both intensity and shape across the emission cone. This discovery would have important ramifications for pulsar statistics, where one of the great uncertainties is the pulsar “beaming fraction”, often guessed at by observing the duty cycles of radio pulsars. Various arguments have been made in favour of both meridional compression (Biggs 1990) and the elongation of pulsar beams (Narayan & Vivekanand 1983), making the actual measurement very important.

In the future it seems as though we will have a much larger number of relativistic systems with which to both test General relativity and map pulsar emission cones. Recent surveys have been finding relativistic pulsars at a welcome rate (Faulkner et al. 2004) and the total pulsar population now exceeds 1500 objects. In particular, the Parkes multibeam surveys have discovered a large number of pulsars in relativistic orbits. The spectacular “double pulsar” is a 2.4 hour binary with two active pulsars, and a geodetic precession period of just 80 years (Lyne et al. 2004). Faulkner et al. (2005) report the recent discovery of the 7.7-hour binary pulsar J1756–2251 with an eccentricity of 0.18 that almost certainly consists of two neutron stars.

The first relativistic binary pulsar discovered by the multibeam surveys was however the 4.8 hour binary pulsar J1141–6545 (Kaspi et al. 2000a). This pulsar orbits what is most likely a white dwarf companion, but the system is unique in that it still possesses a significant orbital eccentricity ($e = 0.17$). An eccentricity of this magnitude suggests that the system was put in its final configuration in an explosive event that may have given the pulsar a significant kick. Recent timing of the system is consistent with a $1.3 M_{\odot}$ pulsar orbiting a $1.0 M_{\odot}$ white dwarf companion (Bailes et al. 2003). It is likely that the system originated as a binary containing two main sequence stars, both below the critical mass required for a supernova. The initially more massive star begins to transfer matter onto its companion as it evolves, causing it to exceed the critical mass. If the system remains bound after the resulting supernova, a young neutron star is left orbiting a white dwarf companion. In the case of symmetric supernovae, the eccentricity of the orbit is induced by the sudden mass loss, and allows us to determine the pre-supernova mass uniquely (Radhakrishnan & Shukre 1985). This ejected mass can be related to the expected runaway velocity of the system, which in the case of PSR J1141–6545, is less than 50 km s^{-1} .

Significant progress has been made in understanding the geometry and location of PSR J1141–6545 through a range of timing and spectroscopic studies. Ord et al. (2002a) demonstrated via HI absorption analysis that the pulsar is at least 3.7 kpc distant. In addition, PSR J1141–6545 was the first pulsar to exhibit dramatic changes in its scintillation time scale as a function of orbital phase, which have enabled an independent estimate of both its orientation and velocity. Ord et al. (2002b) used the orbital modulation of the scintillation time scale to calibrate the usually unknown scale factor that relates the scintillation time scale, scattering screen distance and intrinsic motion to pulsar velocity. Their subsequently determined space motion was greater than that expected from a symmetric supernova (Ord et al. 2002b).

Several years ago we commenced an observing campaign of PSR J1141–6545 to study its HI, scintillation and timing properties over long baselines. It was clear that such observations could also be used to search for relativistic effects such as orbital decay and precession. The DM of the pulsar is 116 pc cm^{-3} , and its scintillation properties are well understood. Ord et al. (2002b) showed that the scintillation bandwidth is much smaller than the 256 MHz observing band used by the analogue filter bank at the Parkes radio telescope, resulting in fairly stable fluxes when integrated over the 4.8 hr orbit.

In this paper we demonstrate that PSR J1141–6545 is undergoing rapid secular evolution of both its total intensity and polarimetric profiles in a manner consistent with geodetic precession. In section 2 we describe the many instrumental systems used to observe this pulsar since its discovery in 1999, along with the associated data reduction methods. Section 3 describes the parameters of the binary system in greater detail and includes a calculation of the expected precession rate. It also introduces two polarimetric profiles that are considerably different from each other, providing the first evidence of profile evolution. Section 4 describes in detail the observed secular changes in the total intensity profile. Polarimetric evolution is considered in section 5, which shows that there has been a convergence of the linear and circular components of the pulsar profile in the last twelve months and that the slope of the position angle swing is steepening, presumably as we approach the emission pole of the pulsar. Finally, in section 6 we discuss the implication of our observations for pulsar surveys and pulsar emission models.

2. Observations

Observations were made at the Parkes radio telescope between July 1999 and May 2004, at centre frequencies ranging from 1318.25 MHz to 1413.50 MHz. Two different receiver packages were used to record data during this period; the central beam of the Parkes multibeam

receiver and the wide band H-OH receiver. The multibeam receiver (Staveley-Smith et al. 1996) has a system temperature of approximately 21K at 20 cm, which was about 5 degrees cooler than the H-OH receiver before it was upgraded near the end of 2003. Flux calibration of both systems using the radio galaxy 3C218 (Hydra A) suggests that the post-upgrade difference is only one or two degrees Kelvin. Our data were recorded with three different instruments, each designed for high time resolution observations across the widest possible bandwidths. Due to the rapid development of digital electronics within the past decade, each new observing system differed significantly from its predecessor.

The Caltech Fast Pulsar Timing Machine (FPTM), described by Navarro (1994), was a hardware-based auto-correlation spectrometer that performed incoherent dedispersion of dual orthogonal polarisations across two bands, each 128 MHz wide. Although the sampling rate was high enough to observe millisecond pulsars (MSPs) with only a few microseconds of smearing (at low DM), this instrument suffered from a number of artifacts induced by radio frequency interference and some deterioration in the correlator boards themselves. In some pulsars this led to oscillations in the passband that contaminated the pulsar profile. Nevertheless, many observations with this instrument were not affected by these problems and it successfully timed many MSPs to high accuracy (Toscano et al. 1999). The FPTM 2-bit sampled the raw data and formed auto-correlation functions that were binned at the apparent spin period of the pulsar. We were able to apply routine 2-bit corrections to enable accurate polarimetry. Being an incoherent detector with a finite number of lags, the FPTM could divide the passband into $4 \times 128 \times 1$ MHz channels, leaving a residual dispersion smear (t_{smear}) given by Eq 1.

$$t_{\text{smear}} = 8.3 \frac{BDM}{\nu^3} \mu\text{s} \quad (1)$$

Here, the channel bandwidth B is in units of MHz, the sky frequency ν is in units of GHz and the dispersion measure DM is in units of pc cm^{-3} . For the configuration used to observe PSR J1141–6545, this corresponds to 350 μs of smearing in the detected pulse profile. Given that the FPTM uses 1024 phase bins across a single pulse period and that PSR J1141–6545 rotates once every 394 ms, each phase bin represents 384 μs of time. The detrimental effects of dispersion smearing are therefore confined to within a single phase bin.

However, if the pulsar spin period is two orders of magnitude shorter (as is typical of the millisecond pulsar population), dispersion smearing can significantly reduce the resolution of an incoherent detector. Motivated by a desire to overcome this problem for MSPs, the Caltech Parkes Swinburne Recorder Mk I (CPSR1) was commissioned in 1998 August. This system implemented a technique called coherent dedispersion (Hankins & Rickett 1975),

which requires Nyquist sampling of the observed band, followed by deconvolution with a response function characteristic of the interstellar medium (ISM). While this approach effectively eliminates dispersion smearing in the detected profiles, it is highly computationally intensive both in terms of the initial data rate and subsequent analysis. CPSR1 streamed digital samples to a striped set of four DLT drives (analogous to the method implemented for the S2 VLBI recorder) whose tapes were shipped to the Swinburne Centre for Astrophysics and Supercomputing for processing. Even with four striped tape drives, CPSR1 was limited to a bandwidth of 20 MHz. Rapid advances in consumer digital electronics soon made it feasible to upgrade the capabilities of the system and in 2002 August, CPSR Mk II was installed at Parkes. CPSR2 performs coherent dedispersion in near real-time, using a cluster of 30 server-class computers located at the telescope. It is capable of recording 2×64 MHz dual-polarisation bands simultaneously, providing a total bandwidth comparable to that of the previous generation of incoherent detectors, like the FPTM. The coherent dedispersion method employed by both CPSR machines allows essentially arbitrary spectral resolution and reduces the dispersion smearing in each channel to a minute fraction of PSR J1141–6545’s period, giving an effective sampling time of a few microseconds.

Individual observations of PSR J1141–6545 ranged in duration from a few minutes to several hours. In recent years, our strategy has been to maximise orbital phase coverage by observing in concentrated sessions during which the pulsar is tracked continuously for two whole orbits (~ 9.6 hr). To calibrate the data we point the telescope one degree south of the pulsar and drive the in-built receiver noise source with a square wave at a frequency of 11.122976 Hz at least once per orbit, to characterise the polarimetric response of the system. In addition, at least once per month we observe the flux calibration source 3C218 (Hydra A).

Our highest density of observations were taken with CPSR2 during 2003 and 2004 (MJD 52845 - 53134), during which time we have a full record of polarimetry, flux and profile morphology. The CPSR1 recorder was designed primarily to observe the bright southern millisecond pulsar J0437–4715 (van Straten et al. 2001), however in 2001 January it took data on PSR J1141–6545 for a total of 30 hours beginning on MJD 51922. The resulting calibrated profile provides important, early epoch information. We have selected three profiles at the widely spaced epochs of MJD 51381, 51781 and 52087, representing high quality FPTM data to further supplement our temporal coverage. It is fortuitous that our earliest FPTM pointing (MJD 51381) dates all the way back to 1999, extending our time baseline by almost two full years. For this reason, we include a 1999 profile despite the fact that the observation was only 12 minutes in duration. Fortunately, PSR J1141–6545 is a bright pulsar with an average flux density of approximately 4 mJy, so the signal-to-noise (S/N) ratio of this 12 minute observations is 125, quite sufficient for our analysis.

All data were processed using the tools included with the PSRCHIVE (Hotan et al. 2004) scheme, with the addition of several extra routines specific to pulse variability analysis¹.

3. PSR J1141–6545

PSR J1141–6545 was discovered in the first Parkes multibeam survey (Kaspi et al. 2000b). It resides in an unusual relativistic binary system, orbiting what is most likely a heavy white dwarf companion once every 4.8 hours. The pulsar does not appear to be recycled and is assumed to be the most recently evolved member of the system. Positioned close to the galactic plane, it is one of the few pulsars whose distance can be estimated by analysis of neutral hydrogen absorption features in its frequency spectrum. Ord et al. (2002a) obtain a lower limit of 3.7 kpc using this method. In addition, the signal from this pulsar exhibits diffractive scintillation over small bandwidths (~ 1 MHz) and time scales of a few minutes (Ord et al. 2002b), which can be used to place timing-independent constraints on the binary parameters. Ord et al. (2002b) report a significant detection of orbital modulation in the observed scintillation velocity (due to the motion of the pulsar in its orbit) and infer both a relative velocity of ~ 115 km s⁻¹ and an orbital inclination angle $i = 76 \pm 2.5^\circ$. This velocity is large compared to the value of < 50 km s⁻¹ expected to result from a symmetric supernova. Uncertainties in our knowledge of the true distance to the pulsar, and hence the relative velocity of the Earth’s standard of rest, combined with uncertainties introduced by the Earth’s orbital motion and bulk flows or anisotropies in the ISM, mean that we cannot convincingly state that the pulsar has an anomalous velocity due to an asymmetric supernova. However, if the profile evolution reported here is due to spin and orbital angular momentum misalignment and geodetic precession, we would expect the pulsar to have received a kick at birth, which would increase its runaway velocity over that of a symmetric explosion.

The rotation period of PSR J1141–6545 is 394 ms, so the precision obtainable through pulse timing experiments is somewhat limited when compared to results (van Straten et al. 2001) obtained by timing millisecond pulsars, whose spin periods are of order 100 times shorter. Despite this, several post-Keplerian parameters are measurable. Bailes et al. (2003) describe a timing solution that includes significant detections of periastron advance ($\dot{\omega} \sim 5.3^\circ$ yr⁻¹), combined transverse Doppler and gravitational redshift (γ) and a marginal detection of orbital period derivative (\dot{P}_b). Despite the lack of any Shapiro delay measurement, we can still derive a good estimate of the component masses. The post-Keplerian parameters $\dot{\omega}$ and γ are related to the pulsar mass (m_p) and companion mass (m_c) by Eq 2 and Eq 3 respec-

¹All PSRCHIVE code is freely available for academic use, see <http://astronomy.swin.edu.au/pulsar>

tively. In addition, pulse timing accurately determines the quantity, derived from Newtonian gravitation, known as the mass function (Eq 4). These equations allow determination of the inclination angle and component masses.

$$\dot{\omega} = 3 \left(\frac{2\pi}{P_b} \right)^{5/3} \left(\frac{G(m_p + m_c)}{c^3} \right)^{2/3} (1 - e^2)^{-1} \quad (2)$$

$$\gamma = e \left(\frac{P_b}{2\pi} \right)^{1/3} \frac{G^{2/3}}{c^2} m_c (m_p + 2m_c) (m_p + m_c)^{4/3} \quad (3)$$

$$f(m_p, m_c) = \frac{m_c^3 \sin^3 i}{(m_p + m_c)^2} = \frac{4\pi^2 a^3 \sin^3 i}{G P_b^2} \quad (4)$$

Here, G is Newton’s gravitational constant, P_b is the pulsar orbital period and $a \sin i$ is the projected semi-major axis. According to Bailes et al. (2003), $m_p = 1.30 \pm 0.02 M_\odot$ and $m_c = 0.986 \pm 0.02 M_\odot$. The timing-derived inclination angle limit ($i > 75^\circ$) compares well with the value obtained from scintillation experiments (Ord et al. 2002b).

Assuming that General relativity is the correct theory of gravity, Barker & O’Connell (1975) present an expression (Eq 5) for the expected, time-averaged precession rate of the pulsar spin axis, Ω_p .

$$\Omega_p = \frac{1}{2} \left(\frac{G}{c^3} \right)^{2/3} \left(\frac{P_b}{2\pi} \right)^{-5/3} \frac{m_c (4m_p + 3m_c)}{(1 - e^2)(m_p + m_c)^{4/3}} \quad (5)$$

Here, c is the speed of light and e is the eccentricity of the system. For PSR J1141–6545, this evaluates to an intrinsic precession rate of $1.36^\circ \text{ yr}^{-1}$, which implies a precession period of 265 years.

Bailes (1988) showed graphically that the maximum observable rate of precession may be significantly less than the intrinsic value. The geometry of the system and our viewing angle have a significant impact on our ability to detect geodetic precession. The observable quantity is the rate at which the angle δ between the observer’s line of sight and the pulsar spin axis changes, as this will manifest itself as a changing cut through the emission cone. Bailes (1988) and Cordes et al. (1990) present expressions for the rate of change of δ , of the form reproduced in Eq 6. The most important parameters in the expression are the misalignment angle between the spin axis and the orbital angular momentum vector, and the precessional phase at the current epoch, neither of which are known.

$$d\delta/dt = \Omega_p \mathbf{n} \cdot (\mathbf{s} \times \mathbf{j})(1 - [\mathbf{n} \cdot \mathbf{s}]^2)^{-1/2} \quad (6)$$

Here, \mathbf{n} is a unit vector along the line of sight to the observer, \mathbf{s} is a unit vector along the pulsar spin axis and \mathbf{j} is a unit vector in the direction of the orbital angular momentum. To evaluate this equation, we must know the misalignment angle, the current precessional phase and the orbital inclination angle i . The first two parameters are unknown for the PSR J1141–6545 system, but we can assume the value of i derived from scintillation studies and plot one precessional period of $d\delta/dt$ for various misalignment angles (see Fig 1).

Unfortunately, it is difficult to translate an observed difference in mean pulse profile morphology into a quantitative measure of angular shift. This requires knowledge of the intrinsic beam shape, which of course we do not possess, making the result model dependent. It is possible that polarimetric studies may offer a key alternative method, however it is still necessary to assume some model of pulsar polarisation as a function of impact angle. In this paper we restrict ourselves, where possible, to a quantitative description of the observed evolution of the mean pulse profile.

3.1. Selected Observations

Fig 2 shows a coherently dedispersed, polarimetrically calibrated mean profile, observed with the multibeam receiver and CPSR1 at a frequency of 1413 MHz in 2001 January (MJD 51922). The pulse profile is morphologically quite simple, consisting of a single component flanked on the left by a shoulder of emission. Note the small “bump” high on the leading edge of the profile, which is also present in the FPTM and analogue filter bank data. The peak fractional polarisation is of order 20 percent in both linear and circular. The position angle swing does not seem to fit the predictions of the rotating vector model and is similar to that seen by Kaspi et al. (2000a), although lacking the orthogonal mode change that is present in the leading shoulder of the Kaspi et al. profile.

Fig 3 shows our most recent fully calibrated mean profile, observed in 2004 May (MJD 53134) with the H-OH receiver and CPSR2, at a centre frequency of 1341 MHz. There are a number of striking differences when compared to Fig 2, most notably an overall broadening of the profile, which now has an extended trailing component; loss of the leading “bump” and general steepening of the position angle swing, which now has an identifiable slope.

Pulsar profiles can be corrupted by systematic errors associated with instrumentation. Typical effects include baseline artifacts due to improper binning and radio frequency interference, insufficient quantisation capabilities in the samplers (leading to the removal of

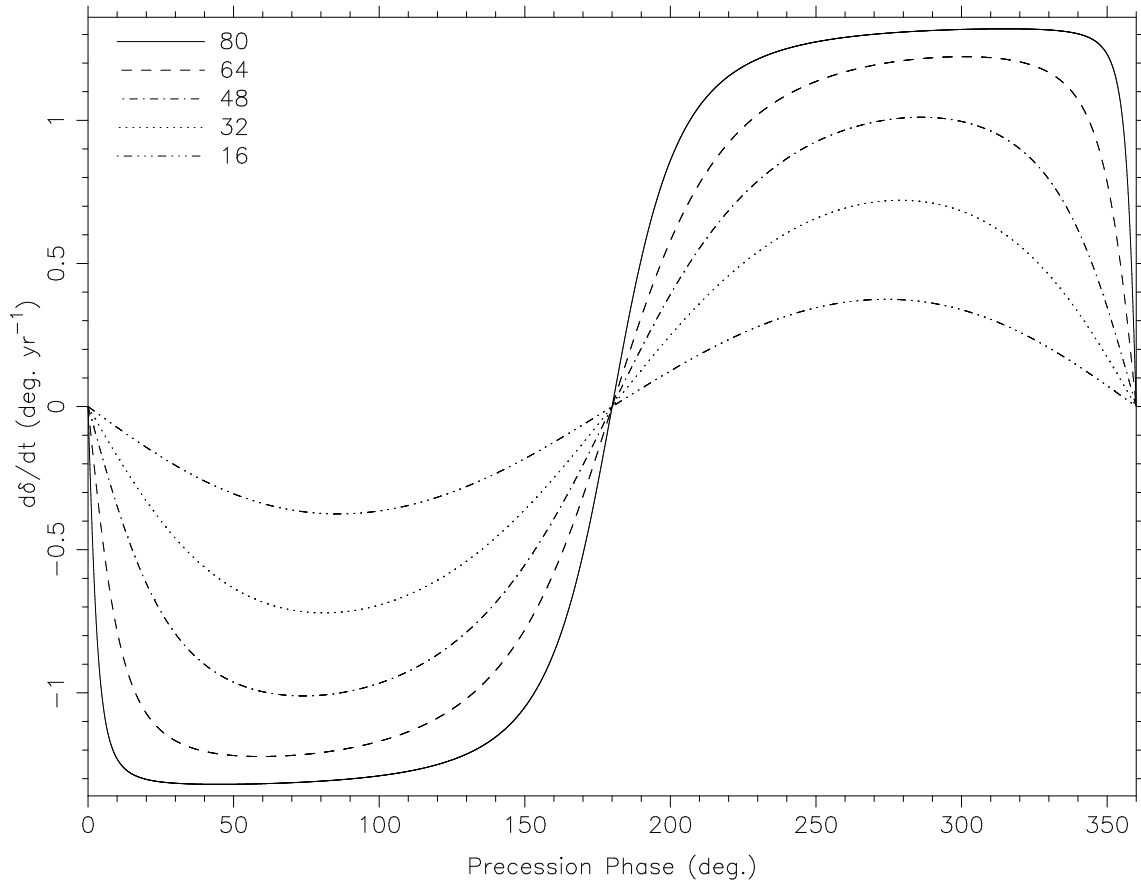


Fig. 1.— Rate of change of the angle between our line of sight and the spin axis of the pulsar ($d\delta/dt$) as a function of precessional phase, for various misalignment angles (shown inset top left, in degrees) for PSR J1141–6545. We have assumed an inclination angle of 76 degrees, consistent with scintillation measurements. The amplitude of the observable precession signature is highly dependent on both the misalignment angle and our current position in the precession cycle, but any derived value of $d\delta/dt$ gives a minimum misalignment angle for the system.

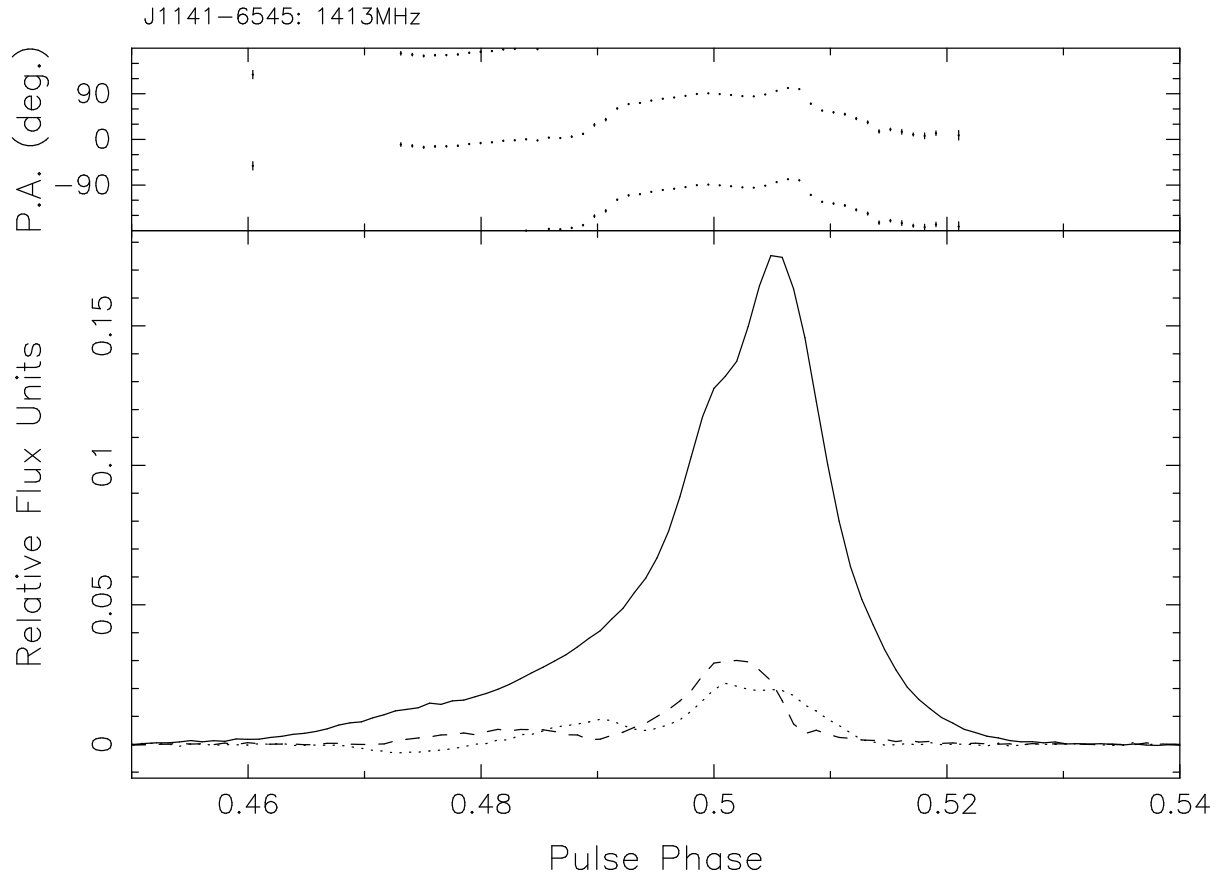


Fig. 2.— PSR J1141–6545 mean profile, obtained from 28 hours of data taken in 2001 January (MJD 51922), at a centre frequency of 1413 MHz. The solid line represents total intensity, the dashed line total linear and the dotted line total circularly polarised emission. There are 1024 phase bins across the profile, which has been polarimetrically calibrated using a simple model of relative gain and phase in the orthogonal linear receiver probes. Note the slight “bump” on the leading edge of the profile and the absence of any steep position angle evolution across the phase range shown.

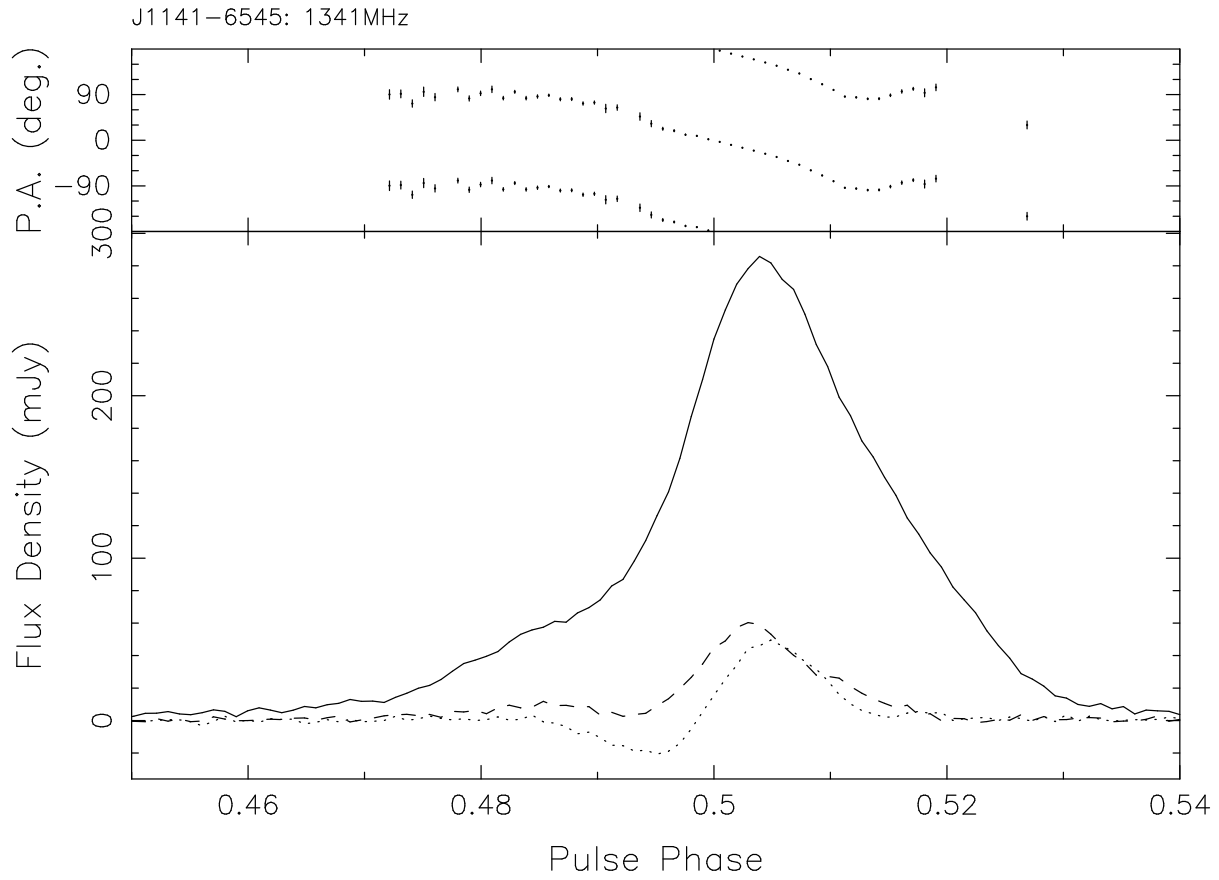


Fig. 3.— 2004 May (MJD 53134) PSR J1141-6545 profile (as in Fig 2) obtained from 2 hours of data taken with CPSR2 at a centre frequency of 1341 MHz. Note the smooth leading edge and extended trailing component, as well as the more pronounced position angle sweep.

power near the pulse as the samplers attempt to maintain an optimum mean level), and smearing due to insufficient time and frequency resolution. Fortunately, in the case of PSR J1141–6545 we have a variety of instruments, each of which has sufficient time resolution to over-sample the profile, and that give self-consistent results at similar epochs. We would be concerned if observed changes only coincided with equipment upgrades, but this has not been the case.

The mean pulse profile has changed significantly in the space of three years. This is confirmed in the next two sections where we present an analysis of data taken during (and before) the epochs presented in Figs 2 & 3. We observe a smooth secular change in the characteristics of the mean pulse.

4. Evolution of the Total Intensity Profile

To examine the evolution of PSR J1141–6545’s mean pulse profile in greater detail, we sum all the data within each observing session to produce a set of 13 well spaced, high S/N profiles. These mean profiles typically span one or two days, with total integrated times of a few hours. Table 1 summarises the most important parameters of each profile including observing system, start date, observing frequency and S/N.

We demonstrate that even though our points are not evenly spaced in time, the data describe a clear trend in profile evolution (Figs 4 & 5). The changes are so great that visual inspection of the profiles can reveal much qualitative information including an overall broadening, extension of the trailing shoulder and smoothing of the leading edge (Fig 4). In addition, we compute a quantitative measure of the width of each mean profile using an algorithm that defines thresholds in pulse phase based on where the flux under the pulse exceeds 10 percent of the peak value for the first time, and drops below this value for the last time. We choose the 10 percent threshold because it includes the majority of the on-pulse region, thus incorporating the important leading and trailing components of the pulse, which are seen to evolve significantly. The secular trend remains if the level is set to 50 percent, however the χ^2 of the linear fit worsens marginally as we would expect from this narrower region of the profile.

A simple linear least-squares fit to the width data shows that the rate of profile broadening is well approximated by a straight line with slope 1.3 ± 0.06 ms yr⁻¹. Unlike PSR B1913+16, PSR J1141–6545 has only a single pulse profile component. It is therefore difficult to constrain the angular extent of the beam, or the angle between the magnetic axis and the line of sight, using total intensity information alone. A similar total intensity profile

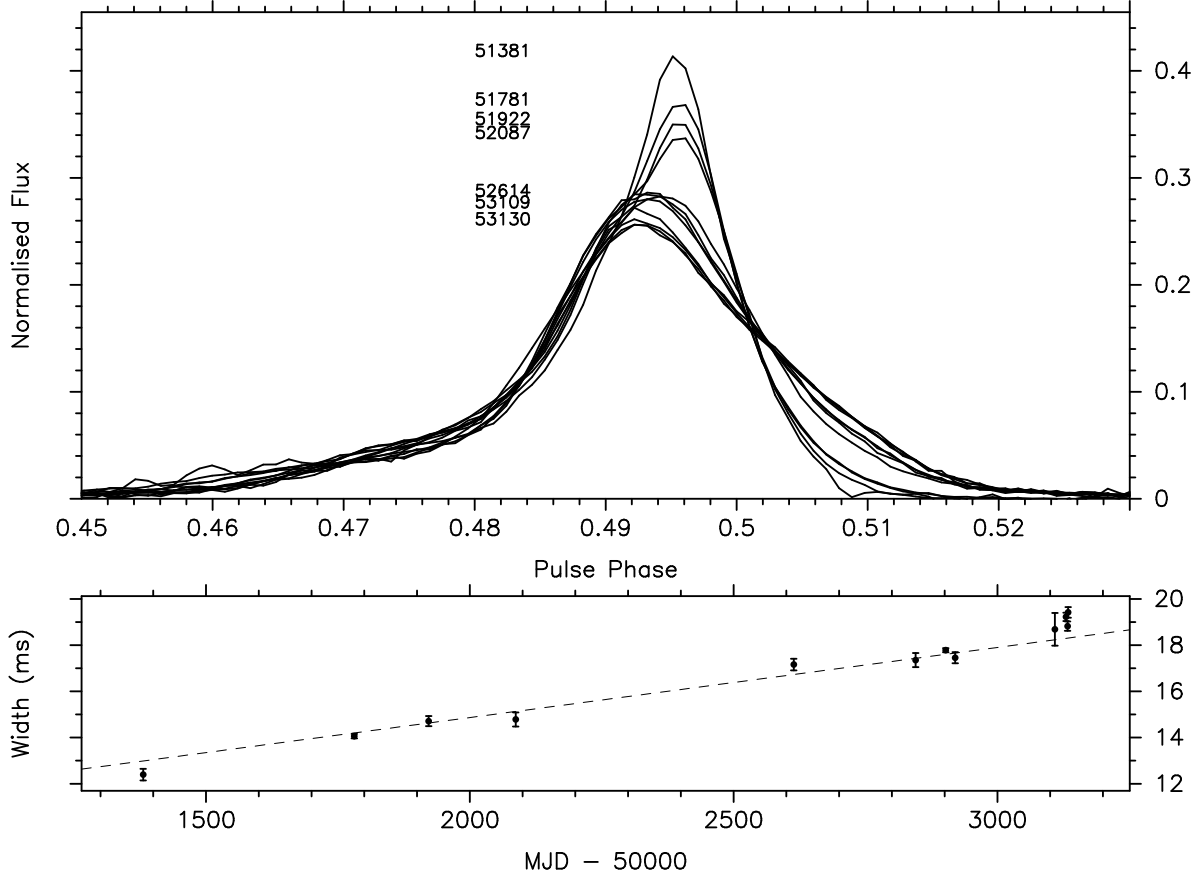


Fig. 4.— The upper panel shows superposed mean total intensity profiles from observations taken at various epochs during the past five years. Each profile was observed at a wavelength near 20cm. The MJD of each observation is marked on the plot, in line with the peak of the corresponding profile. For example, at pulse phase 0.495, the MJD of each observation increases monotonically with decreasing amplitude. The flux under each profile in the plotted region has been normalised to the flux under the earliest profile to allow direct comparison, regardless of the amplitude scaling schemes used by individual instruments. Each mean profile was aligned using an ephemeris obtained from a global timing solution across the entire data set, effectively maximising the cross-correlations between each profile. The lower panel shows the evolution of 10 percent width (see text) as a function of time, with one point for each profile in the upper panel. The profile clearly broadens over the span of our observations. Error bars are derived from consideration of the root-mean-square (RMS) noise level in each profile and represent $1\text{-}\sigma$ uncertainties. The line of best fit, obtained using a linear least-squares method, is shown (dashed).

can be produced by intersecting the centre of a narrow beam or the edge of a wider beam, which introduces a degeneracy in the interpretation. Stairs et al. (2004) describe a method for determining the full geometry of the system through the detection of a secondary precession effect caused by orbitally modulated aberration. Unfortunately we have been unable to detect this in PSR J1141–6545. Given a sufficient time baseline, the profile variations should eventually deviate from the currently observed linear trend. This will also provide an opportunity to constrain the three dimensional geometry of the pulsar system.

In order to characterise the rate of change in more detail, we perform a difference profile analysis on our data set. This involves using (arbitrarily) the first profile in the series as a standard template whose amplitudes are subtracted from the remaining profiles after their flux and alignment have been normalised to the standard. Measurement of the remaining flux in the difference profile gives an indication of how much the profiles vary across a particular epoch (Fig 5). This method is similar to the technique of principle component analysis performed on PSR B1534+12 by Stairs et al. (2004), where only the mean profile and one orthogonal component are taken into account. We use this numerical measure of profile difference to examine quantitatively the rate at which evolution is occurring.

Fig 5 shows that the fractional difference trend is well approximated by a straight line with slope $2.4 \pm 0.07 \times 10^{-4}$ fractional difference units per day. The mean pulse profile of PSR J1141–6545 is therefore changing at a steady rate of approximately 9 percent per year. The profile evolution seen in Figs 4 & 5 is unlikely to be instrumental in origin because it occurs smoothly over the entire time span, instead of jumping discontinuously at the points when new hardware was introduced. In addition, the instrumental upgrades always decreased systematic smearing of the observed profile, whereas we observe the profile width increasing with time.

Given that our observations span a frequency range of almost 100 MHz, it is possible that intrinsic evolution of the profile shape with frequency might contaminate the result. Such contamination is however unlikely to be responsible for the observed secular trend in pulse width, because as Table 1 shows, the changes in observing frequency have not been linear in time. To demonstrate that PSR J1141–6545 does not exhibit significant profile evolution over the range of observing frequencies in our data, we compare two CPSR2 profiles observed on the same day (MJD 53204) in July 2004. These two profiles were observed at 1405 MHz and 1341 MHz respectively and we analyse them in a similar fashion to Fig 5, using the 1405 MHz profile as a standard template and constructing a difference profile. Fig 6 shows that the profile does not evolve significantly across a bandwidth of 64 MHz, therefore we can be confident that frequency evolution does not contaminate our result.

A number of different authors have reported observing the mean profile of a pulsar

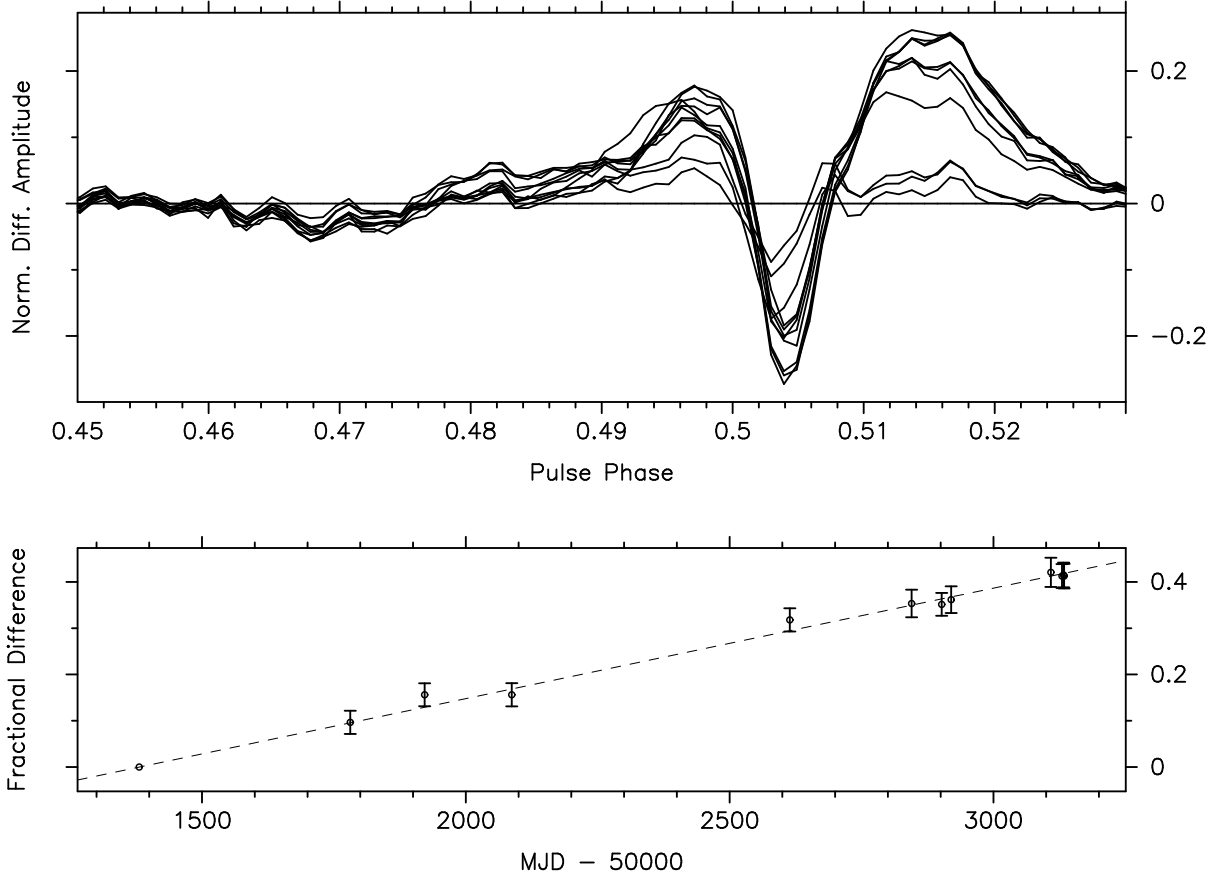


Fig. 5.— The upper panel shows superposed difference profiles, constructed from the data shown in Fig 4, using the earliest profile as a standard template (shown as a horizontal line through zero). The vertical scale is in units of the standard profile flux, indicating that some individual components of the profile have changed by up to 20 percent. There is a monotonic increase in difference amplitude with time, at pulse phase 0.515 for example, the amplitude increases with the MJD of the observation. The lower panel shows the fractional difference between each difference profile and the standard template, as a function of time. Each point represents a single difference profile. The fractional difference is found by summing the absolute values of the amplitude in each pulse phase bin in the difference profile and dividing by the flux in the standard template. Errors are based on measurements of the off-pulse RMS. Whilst this technique is sensitive to changes in S/N as well as morphology, we are confident that our choice of high S/N observations and a narrow phase window allows the morphological information to dominate. The line of best fit is shown (dashed), obtained using a linear least-squares method. Note that the earliest profile has a fractional difference (and error) of zero, providing a reference point.

Instrument	Date (MJD)	Freq (MHz)	S/N
FPTM	51381	1318.25	125
FPTM	51781	1413.50	791
CPSR1	51922	1413.00	778
FPTM	52087	1413.50	743
CPSR2	52614	1405.00	1051
CPSR2	52845	1341.00	427
CPSR2	52902	1341.00	822
CPSR2	52902	1341.00	1354
CPSR2	52920	1341.00	390
CPSR2	53109	1341.00	346
CPSR2	53130	1341.00	728
CPSR2	53133	1341.00	537
CPSR2	53134	1341.00	553

Table 1: List of parameters associated with the 13 observations used to characterise the secular evolution of the PSR J1141–6545 mean pulse profile.

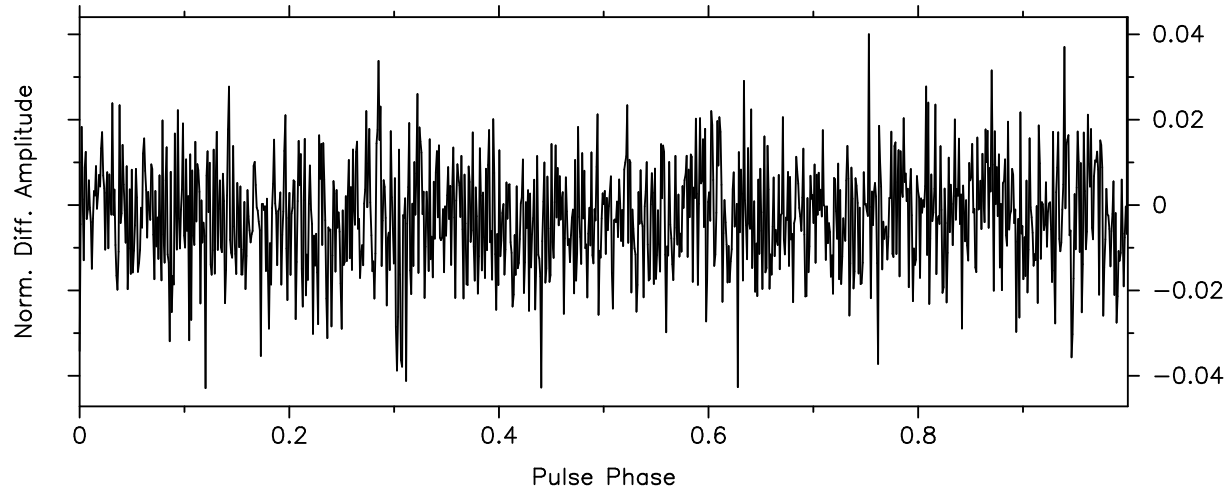


Fig. 6.— Difference profile constructed from two CPSR2 observations taken on MJD 53204 at two frequencies separated by 64 MHz. There is no systematic morphological difference above the level of the noise that might be expected if the pulsar profile was rapidly evolving as a function of radio frequency.

changing in some way. Some slower pulsars have been observed to emit in two or more “modes” of pulse shape, that each remain stable for a time before switching rapidly to another mode (Lyne 1971). In more recent years, various authors have reported observing random profile variations in some of the millisecond pulsars, most notably PSR B1821–24 (Backer & Sallmen 1997) and PSR J1022+1001 (Kramer et al. 1999). None of the reported variations, or the mode changing phenomenon, match the steady secular change we have observed in PSR J1141–6545, which is itself a slow pulsar and therefore may not suffer from the erratic variations seen in a small number of the millisecond pulsars. It is still unclear whether or not random variations in MSP profiles are intrinsic to the pulsar as a recent analysis of PSR J1022+1001 observations made by Hotan et al. (2004) finds no instabilities that might induce strange timing behaviour.

Can we hope to distinguish between geodetic precession and, say, free precession of the pulsar? Pulse shape variations are attributed to free precession in observations of PSR B1828–11 (Stairs et al. 2000) and PSR B1642–03 (Shabanova et al. 2001). This evidence manifests in the form of profile shape changes correlated to variations in the pulse arrival times. These changes are cyclic, but with no clear *a priori* time scale. The geodetic precession time scale is already well determined to be near 265 years. From Fig 1. we would hope to see the emission cone tilt at a rate $< 1.36 \text{ deg yr}^{-1}$ and continue any secular trend for decades unless we are at one of the two crossing points encountered every geodetic precession period. The overwhelming majority of slow pulsars exhibit no evidence for free precession whatsoever. On the other hand, we expect any binary pulsar that has received a misaligning kick to precess to some degree. We therefore assert that geodetic precession is responsible for the observed secular variation in the mean profile of PSR J1141–6545 and we discuss this interpretation in section 6. Long-term monitoring of the precession will ultimately determine a time scale and hence the true mechanism.

We now present an analysis of the polarimetry of this pulsar, providing further evidence that our line of sight to the emission cone is changing steadily with time.

5. Evolution of Polarised Emission

The standard interpretation of pulsar polarimetry is the rotating vector model (RVM), put forward by Radhakrishnan & Cooke (1969). This assumes a dipolar magnetic field whose central axis is offset from the neutron star rotation axis. As the emission cone sweeps past our line of sight, the changing orientation between the observer and the magnetic field is expected to produce a characteristic “S” shaped curve in the measured position angle of any linearly polarised components. In addition, the rate at which the linear polarisation vector

rotates as the beam crosses the observer is dependent on whether or not the line of sight cuts close to the centre of the beam. Polarimetric observations may therefore offer a sensitive indicator of both the rate at which the beam is precessing past the observer and where in the emission cone we are at the present time.

First we consider the morphology of the polarised component of the mean pulse. The polarimetric changes observed between Figs 2 & 3 are extreme. To convince ourselves that rapid polarimetric evolution is taking place, we focus on the most recent data with a high time density of observations and the same pulsar back-end (CPSR2). The polarimetric capabilities of CPSR2 and the PSRCHIVE scheme (Hotan et al. 2004) have recently been verified by comparison with published results with good agreement (Ord et al. 2004). Fig 7 shows profiles of the polarised emission of PSR J1141–6545, recorded using CPSR2 and ordered consecutively in time.

Fig 7 shows that the polarimetric profile is certainly changing, even over a period of less than 10 months. The linear and circular emission appears to converge during this time. Significant morphological differences in polarised emission appear between two widely separated observations that also correspond to a change in receiver, when the multibeam system was replaced by the refurbished H-OH. Therefore it is still possible that the differences in polarised emission could be instrumental in origin, although comparison with Fig 2 suggests that position angle evolution is also occurring. Observations over a longer time span are required to make more conclusive (and perhaps quantitative) statements. Regular polarimetric observations of this pulsar will be a high priority in future years.

Next we attempt a more quantitative analysis of the position angle of the linearly polarised component of the pulsar beam. In the formalism of the RVM, measured position angle (PA, ψ), is presented as a function of the angle between the spin and magnetic axes (α), the minimum angle between the magnetic axis and the line of sight (β) and pulse phase (ϕ), as shown in Eq 7.

$$\tan(\psi(\phi) - \psi_0) = \frac{\sin \alpha \sin(\phi - \phi_0)}{\cos \alpha \sin \delta - \sin \alpha \cos \delta \cos(\phi - \phi_0)}, \quad (7)$$

Here $\delta = \alpha + \beta$ is the angle between the spin axis and the line of sight, as in section 3; ϕ_0 is the pulse phase of steepest PA swing and ψ_0 is a constant position angle offset.

Unfortunately, application of this method to pulsars with narrow duty cycles and shallow or complicated PA swings does not well constrain α or β independently. In common with the analysis presented by Kaspi et al. (2000a) we find it impossible to fit the RVM model to the early observations of PSR J1141–6545 with any degree of confidence. More recent

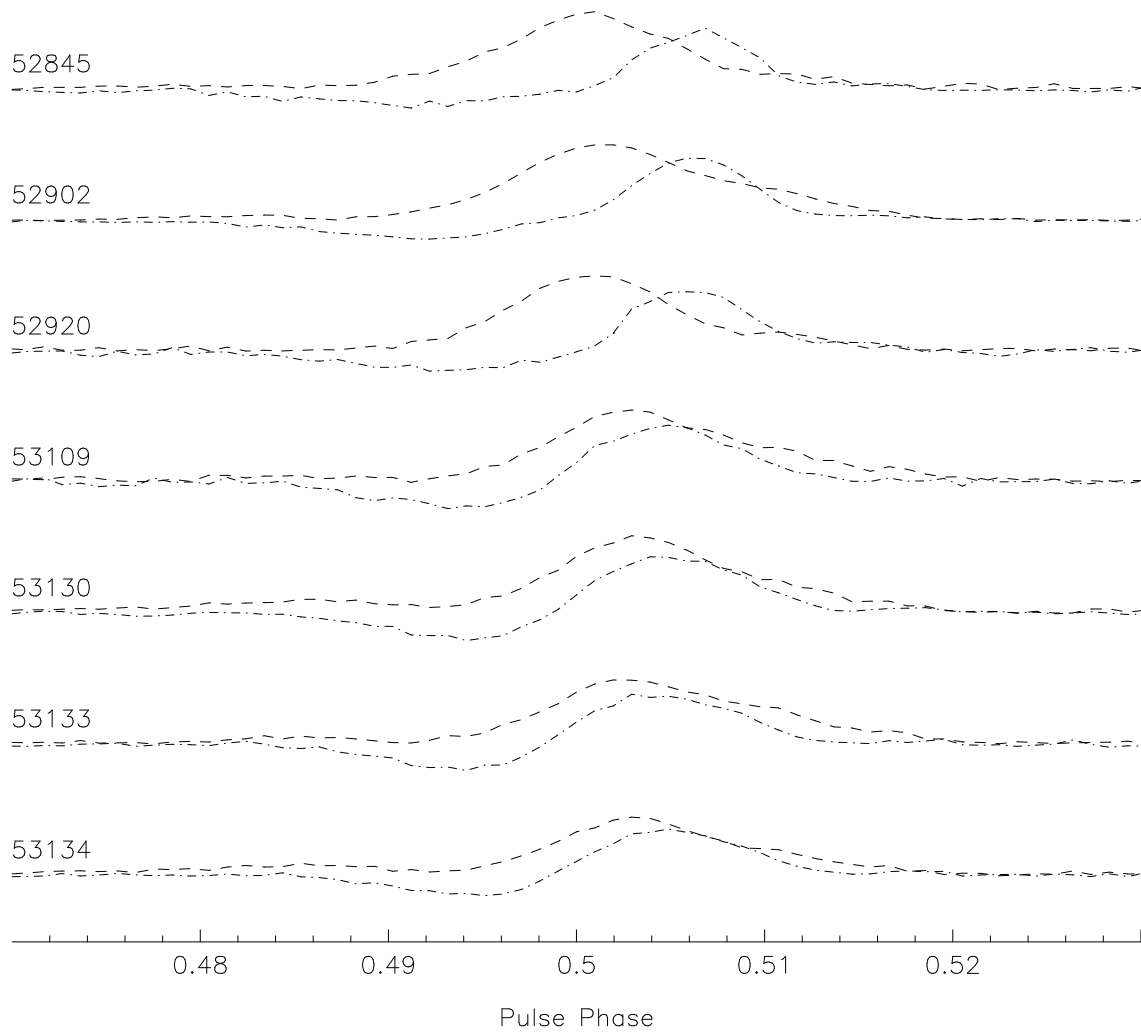


Fig. 7.— Consecutive profiles of the polarised emission from PSR J1141–6545, observed with CPSR2 over a period of 289 days beginning in 2003 July (MJD 52845). The dashed line represents total linear polarisation and the dashed-dotted line represents total circular. The vertical axis (unlabeled for simplicity) is in mJy, the vertical range is kept constant across all sub-panels. All profiles have been polarimetrically calibrated using a simple model of relative gain and phase for two orthogonal linear receiver probes and flux calibrated against Hydra A. The peaks of the linear and circular components can be seen to move closer together as time progresses.

observations are better suited to a partial RVM analysis, in that the recent PA behaviour includes a sweep in the central region of the pulse profile. The narrow duty cycle still restricts the applicability of the RVM and it is therefore impossible to constrain α . Under the assumption that the steepest PA evolution is still providing an indication of the orientation of the magnetic field lines with respect to both the spin axis and the line of sight we have applied a simplification of the RVM model with the sole purpose of determining the general evolution of β . Within the RVM formalism the rate of change of PA as a function of pulse phase has a maximum value, given in Eq 8:

$$\left(\frac{d\psi}{d\phi}\right)_{\max} = \frac{\sin \alpha}{\sin \beta} \quad (8)$$

We have evaluated the gradient of the steepest PA swing in those observations for which a straight line fit can be obtained from the same central region of the pulse profile. This procedure could only be applied to epochs between which the linear behaviour of the PA swing was considerably wider in pulse phase than any possible translation, allowing the profiles to be aligned by a suitable ephemeris. The applicable observations are those obtained with CPSR2 since mid 2003. Earlier observations cannot be subject to this analysis as they display PA behaviour which is too complicated. This fact alone indicates that the detected emission represents a different cut through the emission region than was evident in earlier observations.

The data have been grouped into two epochs (2003 and 2004) separated by approximately 0.7 years. Average position angle profiles were formed from the constituent observations at each epoch. These average PA profiles include observations from both 64 MHz observing bands and within each epoch are separated by several days. Although there were very slight variations between the PA profiles within each epoch, there was no systematic trend. A linear least squares minimisation of a straight line fit to the PA profiles demonstrates a significant deviation in the gradient obtained at the two epochs. Epoch one (2003) displays a gradient of -15.1 ± 0.3 degrees of PA swing per degree of phase. Epoch two (2004) displays a gradient of -17.1 ± 0.3 degrees of PA swing per degree of phase. A straight line fit to a difference PA profile, formed by the subtraction of the epoch two profile from the epoch one profile, is presented in Fig 8. The gradient of this difference fit is 2.3 ± 0.4 , which is consistent with the simple subtraction of the best fit for epoch two from that of epoch one.

Eq 8 was then evaluated for all α and a rate of change of β between the two epochs was determined. The calculated value of $d\beta/dt$ is a strong function of α but suggests that β is increasing. The peak rate of change is $0.8 \text{ degrees yr}^{-1}$ (68 % confidence), but this

interpretation requires the pulsar spin axis to be 90 deg from the magnetic axis, which is unlikely if we assume the orientation is random. It is therefore probable that $d\beta/dt$ is less than 0.8 degrees yr^{-1} . The gradient of PA also indicates that β is currently negative for all possible α . We therefore infer that the beam is precessing into the line of sight at a rate less than 0.8 degrees yr^{-1} . It should be noted that $d\beta/dt \equiv d\delta/dt$ as the two angles are related by a constant offset. Thus we can use this result, coupled with Fig 1, to make some general statements about the unknowns in Eq 6. It is clear that either the misalignment angle is smaller than approximately 30° , or we are currently at a special precessional phase where $d\delta/dt$ is changing rapidly and has not attained its maximum value in the span of our observations. Conversely, unless α is near 0° or 180° , we expect that the misalignment angle is greater than approximately 15° .

The mean flux of the pulsar in these observations is 4.0 ± 0.5 mJy. There does not appear to be a significant trend in mean flux within the past year, but this may change as the time baseline of flux calibrated data grows.

6. Discussion & Conclusion

Our observations indicate that the line of sight to the emission cone of PSR J1141–6545 is precessing deeper into the core, producing a steeper position angle swing. Depending on the chosen beam model, this could also explain why the pulse profile is seen to increase in width. Our result has implications both for the study of pulsar emission beams and for the detection rates of relativistic pulsars in large-scale surveys. PSR J1141–6545 is the slowest pulsar (by an order of magnitude) for which geodetic precession is observable, providing a unique means of examining the emission cone of a normal (un-recycled) pulsar. Further polarimetric observations, extended time baselines or the detection of orbitally modulated aberration may allow determination of our present location in the emission cone and the geometry of the beam as a whole. Given the expected precession period of order 265 years and the fact that we seem to still be moving towards the central axis of the beam, it is possible that this pulsar may only have precessed into view within the past few decades. This might explain its non-detection in early pulsar surveys with flux limits well below the required threshold (Johnston et al. 1992; Manchester et al. 1996). If this is the case, it could be argued that surveys of the sky for relativistic pulsars should continue on a regular basis. By their very nature, the most interesting objects are likely to be visible for the least amount of time.

The Parkes radio telescope is operated by the Australia Telescope National Facility on

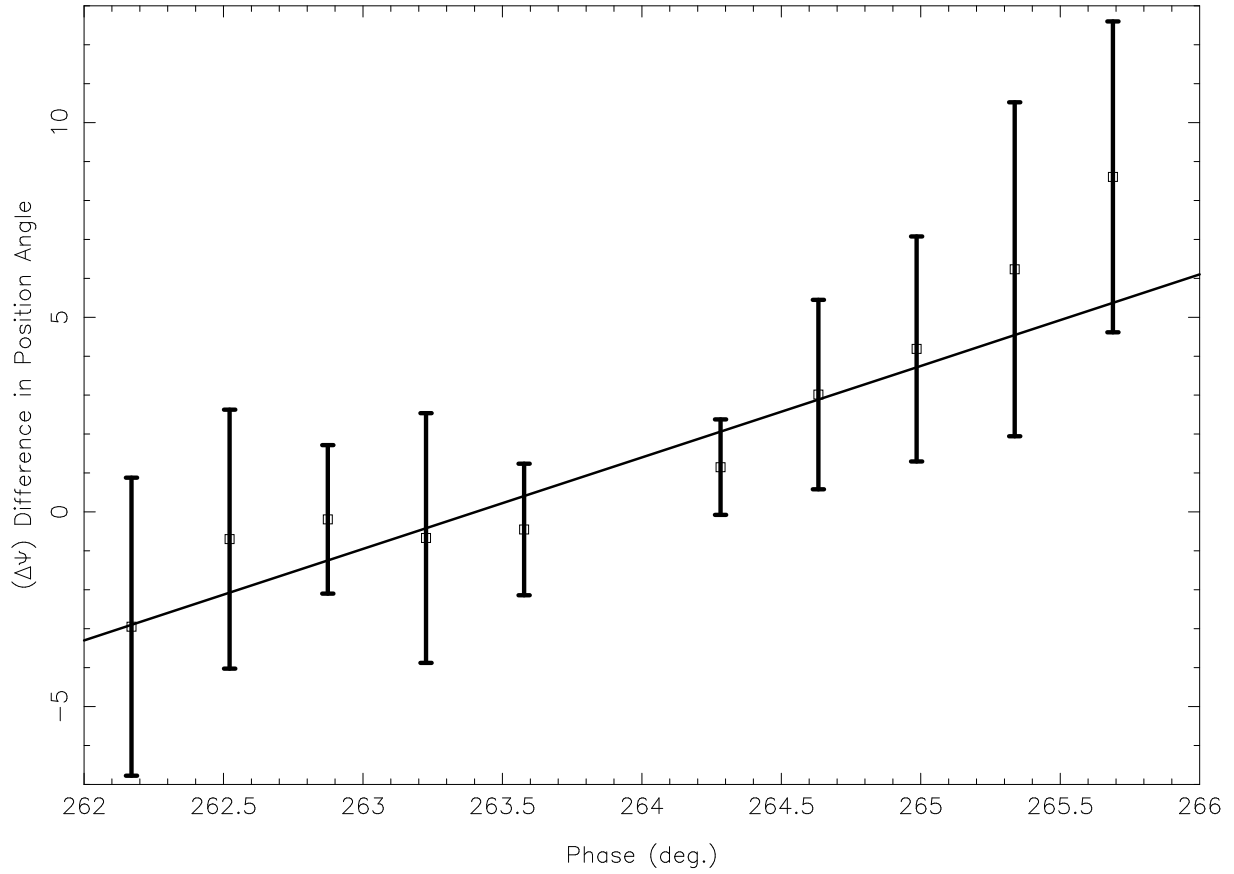


Fig. 8.— The difference position angle (PA) as a function of phase. The average PA from the mid-2004 epoch was subtracted from that of the mid-2003 epoch. A straight line fit has been applied to the residual. The steepening of the PA swing as a function of time is an indication that the pulsar emission beam may be precessing into, and not away from our line of sight.

behalf of the Commonwealth Scientific and Industrial Research Organisation (CSIRO). We are grateful to Ruth Musgrave for assistance with data reduction and Willem van Straten and Haydon Knight for assistance with observations and software development. AWH is the recipient of an Australian Post-graduate Award (APA) and CSIRO top-up allowance and thanks Claire Trenham for support and encouragement.

REFERENCES

- Anderson, S. B., Gorham, P. W., and T. A. Prince, S. R. K., & Wolszczan, A. 1990, *Nature*, 346, 42
- Backer, D. C. & Sallmen, S. 1997, *AJ*, 114, 1539
- Bailes, M. 1988, *A&A*, 202, 109
- Bailes, M., Ord, S. M., Knight, H. S., & Hotan, A. W. 2003, *ApJ*, 595, 49
- Barker, B. M. & O’Connell, R. F. 1975, *Phys. Rev. D*, 12, 329
- Barker, B. M. & O’Connell, R. F. 1975, *ApJ*, 199, L25
- Biggs, J. D. 1990, *MNRAS*, 245, 514
- Cordes, J. M., Wasserman, I., & Blaskiewicz, M. 1990, *ApJ*, 349, 546
- Damour, T. & Ruffini, R. 1974, *C. R. Acad. Sc. Paris, Serie A*, 279, 971
- Esposito, L. W. & Harrison, E. R. 1975, *ApJ*, 196, L1
- Faulkner, A. J., Kramer, M., Lyne, A. G., Manchester, R. N., McLaughlin, M. A., Stairs, I. H., Hobbs, G., Possenti, A., Lorimer, D. R., D’Amico, N., Camilo, F., & Burgay, M. 2005, *ApJ*, 618, 119
- Faulkner, A. J., Stairs, I. H., Kramer, M., Lyne, A. G., Hobbs, G., Possenti, A., Lorimer, D. R., Manchester, R. N., McLaughlin, M. A., D’Amico, N., Camilo, F., & Burgay, M. 2004, *MNRAS*, 355, 147
- Hankins, T. H. & Rickett, B. J. 1975, in *Methods in Computational Physics Volume 14 — Radio Astronomy* (New York: Academic Press), 55–129
- Hari Dass, N. D. & Radhakrishnan, V. 1975, *Astrophys. Lett.*, 16, 61
- Hotan, A., van Straten, W., & Manchester, R. N. 2004, *A&A*, in press

- Hotan, A. W., Bailes, M., & Ord, S. M. 2004, MNRAS, 355, 941
- Hulse, R. A. & Taylor, J. H. 1974, ApJ, 191, L59
- Johnston, S., Lyne, A. G., Manchester, R. N., Kniffen, D. A., D’Amico, N., Lim, J., & Ashworth, M. 1992, MNRAS, 255, 401
- Kaspi, V. M., Lackey, J. R., Mattox, J., Manchester, R. N., Bailes, M., & Pace, R. 2000a, ApJ, 528, 445
- Kaspi, V. M., Lyne, A. G., Manchester, R. N., Crawford, F., Camilo, F., Bell, J. F., D’Amico, N., Stairs, I. H., McKay, N. P. F., Morris, D. J., & Possenti, A. 2000b, ApJ, 543, 321
- Konacki, M., Wolszczan, A., & Stairs, I. H. 2003, ApJ, 589, 495
- Kramer, M. 1998, ApJ, 509, 856
- Kramer, M., Xilouris, K. M., Camilo, F., Nice, D., Lange, C., Backer, D. C., & Doroshenko, O. 1999, ApJ, 520, 324
- Lyne, A. G. 1971, MNRAS, 153, 27P
- Lyne, A. G., Burgay, M., Kramer, M., Possenti, A., Manchester, R. N., Camilo, F., McLaughlin, M., Lorimer, D. R., Joshi, B. C., Reynolds, J. E., & Freire, P. C. C. 2004, Science, 303, 1153
- Manchester, R. N., Lyne, A. G., D’Amico, N., Bailes, M., Johnston, S., Lorimer, D. R., Harrison, P. A., Nicastro, L., & Bell, J. F. 1996, MNRAS, 279, 1235
- Narayan, R. & Vivekanand, M. 1983, A&A, 122, 45
- Navarro, J. 1994, PhD thesis, California Institute of Technology
- Ord, S. M., Bailes, M., & van Straten, W. 2002a, MNRAS, 337, 409
- . 2002b, ApJ, 574, L75
- Ord, S. M., van Straten, W., Hotan, A. W., & Bailes, M. 2004, MNRAS, 352, 804
- Radhakrishnan, V. & Cooke, D. J. 1969, Astrophys. Lett., 3, 225
- Radhakrishnan, V. & Shukre, C. S. 1985, in *Supernovae, Their Progenitors and Remnants*, ed. G. Srinivasan & V. Radhakrishnan (Bangalore: Indian Academy of Sciences), 155–169

- Shabanova, T. V., Lyne, A. G., & Urama, J. O. 2001, *ApJ*, 552, 321
- Stairs, I. H., Lyne, A. G., & Shemar, S. 2000, *Nature*, 406, 484
- Stairs, I. H., Thorsett, S. E., & Arzoumanian, Z. 2004, *Phys. Rev. Lett.*, 93
- Staveley-Smith, L., Wilson, W. E., Bird, T. S., Disney, M. J., Ekers, R. D., Freeman, K. C., Haynes, R. F., Sinclair, M. W., Vaile, R. A., Webster, R. L., & Wright, A. E. 1996, *Proc. Astr. Soc. Aust.*, 13, 243
- Stinebring, D. R., Smirnova, T. V., Hankins, T. H., Hovis, J., Kaspi, V., Kempner, J., Meyers, E., & Nice, D. J. 2000, *ApJ*, 539, 300
- Taylor, J. H. & Weisberg, J. M. 1982, *ApJ*, 253, 908
- Toscano, M., Sandhu, J. S., Bailes, M., Manchester, R. N., Britton, M. C., Kulkarni, S. R., Anderson, S. B., & Stappers, B. W. 1999, *MNRAS*, 307, 925
- van Straten, W., Bailes, M., Britton, M., Kulkarni, S. R., Anderson, S. B., Manchester, R. N., & Sarkissian, J. 2001, *Nature*, 412, 158
- Weisberg, J. M., Romani, R. W., & Taylor, J. H. 1989, *ApJ*, 347, 1030
- Weisberg, J. M. & Taylor, J. H. 2002, *ApJ*, 576, 942
- Wex, N., Kalogera, V., & Kramer, M. 2000, *ApJ*, 528, 401
- Wolszczan, A. 1990, PSR 1257+12 and PSR 1534+12